



Highly efficient and mechanically robust stretchable polymer solar cells with random buckling



Rui Ma ^a, Jing Feng ^{a,*}, Da Yin ^a, Hong-Bo Sun ^{a,b}

^a State Key Laboratory on Integrated Optoelectronics, College of Electronic Science and Engineering, Jilin University, 2699 Qianjin Street, Changchun, 130012, China

^b College of Physics, Jilin University, 119 Jiefang Road, Changchun, 130023, China

ARTICLE INFO

Article history:

Received 5 August 2016

Received in revised form

21 October 2016

Accepted 31 December 2016

Available online 3 January 2017

Keywords:

Polymer solar cell

Stretchable

High efficiency

Mechanically robust

ABSTRACT

Stretchable polymer solar cells have shown great potential as stretchable power generators for applications in stretchable electronics, such as wearable electronics, electronic skins and stretchable displays. However, their mechanical stability and power conversion efficiency (PCE) thus are still far below the requirement for the practical applications. Here, we have developed highly efficient and stretchable polymer solar cells (PSCs) based on a random buckling process. The stretchable PSCs are fabricated by attaching the ultrathin PSC onto a pre-stretched elastomeric substrate and then releasing the prestrain to form random bucklings. Its PCE of 5.8% under 70% tensile strain is the largest to date among the reported PSCs. The stretchable PSCs exhibit small fluctuations in performance after 400 stretching-releasing cycles. This is an important step towards producing stretchable PSCs for commercial applications.

© 2017 Elsevier B.V. All rights reserved.

1. Introduction

Stretchable electronics are a type of mechanically robust electronics represented by next-generation wearable and implantable devices which can be bended, folded, crumpled and stretched [1–5]. In order to facilitate the application of these modern stretchable electronic devices, the highly efficient and stretchable polymer solar cells (PSCs) are one of the best candidates for supplying energy to stretchable electronic devices [6,7]. Construction of common PSCs mainly consists of transparent electrodes, transport layers and absorption layer. For intrinsically stretchable devices, all functional layers must be elastic. However, It has been demonstrated that polymer-fullerene derivative active material films commonly used in PSCs have an elongation at break of only 0.3% [8], so that the intrinsically stretchable PSCs have not been successfully fabricated by far. To overcome the limit of the low ultimate strain of the polymer-fullerene derivative films, mechanical buckling on a rigid film has been developed by applying compressive strain to a pre-stretched elastomeric substrate. Stretchable PSCs based on the mechanical buckling by fabricating the PSCs on a pre-stretched poly(dimethylsiloxane) (PDMS)

elastomer have been demonstrated [9]. However, its strain of 22.2% and PCE of 2.0% were not sufficient to meet the demand of practical applications. Siegfried Bauer et al. presented a stretchable PSCs by fabricating the PSC on an ultrathin PET substrate and attaching it to a pre-stretched adhesive tape to form random buckles [10]. The maximal tensile strain was improved to 400% successfully, and the energy conversion efficiency of 4.0% has been achieved. However, its 22 stretching-releasing cycles was not sufficient for practical applications. The damage to the electrodes of the ultrathin PSCs during the stretching-releasing process caused by its direct contact with adhesive tape is one of the possible reasons for the low mechanical stability. So far, high efficiency and mechanical stability are still challenges for the stretchable PSCs.

On the other hand, flexible transparent conductive electrodes (TCEs) is one of the limitations for the efficient stretchable PSCs. Excellent ductility, high transmittance and conductivity are required for flexible TCEs. Traditional indium tin oxide (ITO) electrode is too friable to be suitable for highly flexible TCEs. Poly(3,4-ethylenedioxythiophene):poly(styrenesulfonate) (PEDOT:PSS) has been used in stretchable PSCs as the flexible TCEs, while its sheet resistances (R_S) is higher than metallic electrodes by one order of magnitude [9,10]. Recently, ultrathin metallic TCEs fabricated on metal oxide layer such as WO_3 , MoO_3 , ZnO with high ductility, transmittance and conductivity are realized and they meet the requirements of the electrodes in the flexible optoelectronic devices

* Corresponding author.

E-mail address: jingfeng@jlu.edu.cn (J. Feng).

TCEs [11–14].

In this work, we demonstrate highly stretchable PSCs with high efficiency and improved mechanical robustness. The PSCs with an ultrathin flexible metallic TCEs were fabricated on an ultrathin photopolymer film and then attached to elastomeric support to form random bucklings. The mechanical stability has been improved by inserting a sacrificial layer between the ultrathin PSC and elastomeric support to avoid their direct contact. The stretchable PSCs exhibit power conversion efficiency of 5.8% under 70% tensile strain state, which is the highest PCE reported to date for the stretchable PSCs to the best of our knowledge. More importantly, the stretchable PSCs exhibit only small fluctuations in performance after 400 stretching-releasing cycles. This simple and low-cost method is compatible with most PSCs fabrication processes, such as thermal evaporation, spin coating, and ink-jet printing, so that it could be applied to more efficient solar cells with complex structures.

2. Experiment details

The pre-cleaned Si substrate was treated with Octadecyltrichlorosilane (OTS) [15] to realize a hydrophobic surface with lowered surface energy, so that the ultrathin PSCs can be peeled off from the substrate completely. The ultrathin photopolymer film (NOA63, Norland Inc.) was spin-coated onto the Si substrate at 12,000 rpm for 90 s and then exposed to an ultraviolet light source for 5 min with a power of 125 W. The thickness of the NOA63 film used as ultrathin flexible substrate was about 2.7 μm . Thicknesses of the NOA63 film were measured using an XP-2 stylus profilometer (Ambios Technology, Inc.). The ultrathin anode composed of a wetting layer of 3 nm MoO_3 , a seed layer of 1 nm Au, a middle layer

of 7 nm Ag and a hole transport layer of 10 nm MoO_3 was deposited on the ultrathin polymer substrate by thermal evaporation in sequence at a vacuum of $<5 \times 10^{-4}$ Pa. The transmission spectra and the sheet resistance of the TCEs were measured by a UV–Vis spectrophotometer (UV-2550, SHIMADZU Co.Inc.) and a four-probe meter, respectively. The SEM images were characterized by a field emission scanning electron microscope (SEM, JSM-7500F, JEOL).

Architecture illustration of ultrathin PSC and schematic illustration of the fabrication process of stretchable PSCs are shown in Fig. 1. The PSCs were fabricated on ultrathin flexible metallic TCEs. First, a solution of PCDTBT and PC_{71}BM (1:4 w/w, polymer concentration of 25 mg/mL) in 1,2-dichlorobenzene was spin-coated on top of the TCE at 3000 rpm for 30 s as the photoactive blend layer. The resulting layer with a thickness of about 80 nm was annealed on a hotplate at 70 $^\circ\text{C}$ for 1 h in the glove box. Then, a cathode of 1 nm LiF, 1 nm Al, 80 nm Ag were thermally deposited on PCDTBT: PC_{71}BM film. Finally, a NPB film with a thickness of 0, 10, 20, 30 and 40 nm was coated on the cathode as a sacrificed layer. Two rigid plastic tapes were adhered to the two opposite sides of the adhesive elastomer (3M VHB 4905) where the distance between the two rigid tapes was exactly 5 mm. The elastomeric substrate was stretched until the distance between the two rigid tapes reached 15 mm by a home-made moving stage. The ultrathin PSC that was peeled off completely from the Si substrate was adhered onto the pre-stretched elastomeric substrate between the two rigid tapes by contacting with NPB sacrificial layer. The active area of the cell was roughly $3 \times 1.5 \text{ mm}^2$, and we aligned the long dimension of devices in the direction of stretching. We defined the length of the device to be L , so the maximum value of L (L_{max}) was 3 mm. We released stress by moving the rigid tapes closer together, allowing the elastomeric substrate to relax, which compressed the

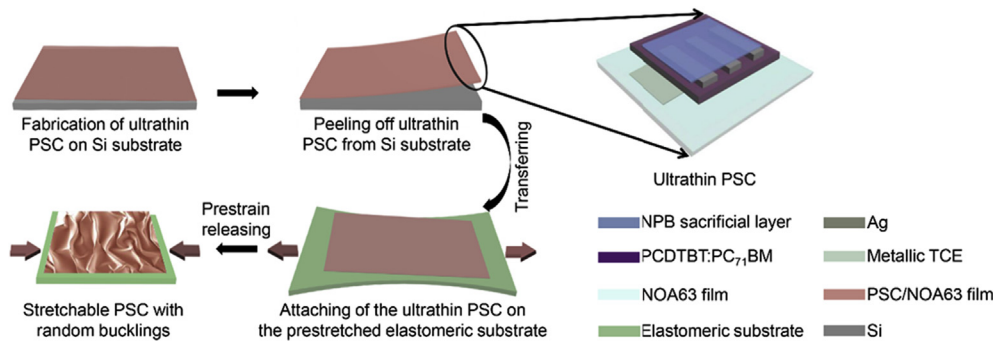


Fig. 1. Schematic illustration of the fabrication process of stretchable PSCs.

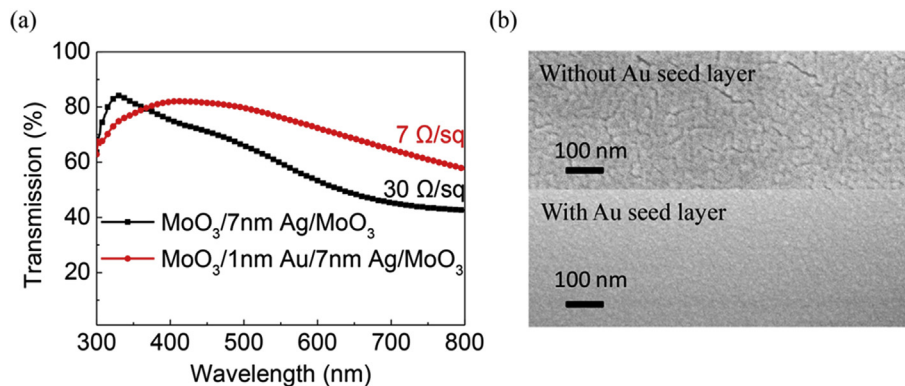


Fig. 2. (a) Transmittance spectra and sheet resistance of the ultrathin flexible TCEs with and without 1 nm Au seed layer. (b) SEM images of the ultrathin flexible TCEs with and without the 1 nm Au seed layer.

device area. When the distance between the two rigid delimiters was 5 mm, the length of devices was L_0 (1.75 mm). Tensile strain was defined to be $(L - L_0)/L_0$, so the maximal tensile strain was about 70%. The photographs of the stretchable devices at 0%, 20%, 50% and 70% strain were taken by a digital single lens reflex camera. Electrical contact was made with copper wires and drops of eutectic gallium-indium at the point where the anode and cathode of the PSCs extended out of the active region of the devices. The PSCs were characterized under illumination of a solar simulator (A.M. 1.5 Global spectrum with a light intensity of 100 mW cm^{-2}). All I-V characteristics were recorded using a Keithley 2400 source meter.

3. Results and discussions

Highly flexible TCEs are required for the stretchable PSCs. Here we chose ultrathin metallic TCE on ultrathin polymer film to replace the commonly-used PEDOT:PSS electrode. The construction of our TCE is MoO_3 (3 nm)/Au (1 nm)/Ag (7 nm)/ MoO_3 (10 nm). A wetting layer of 3 nm MoO_3 and a seed layer of 1 nm Au are usually placed underneath the Ag film to promote the formation of a continuous film below 10 nm. The later MoO_3 layer with a thickness of 10 nm is used both as an anti-reflective layer and a hole transport layer. Fig. 2(a) shows the transmittance spectra of the ultrathin flexible metallic TCEs with and without the Au seed layer. The transmittance can be increased from an average value of 65%–72% by introducing the Au seed layer and it is comparable with the PEDOT:PSS electrode. While the sheet resistance of the ultrathin flexible metallic TCE is decreased from $30 \Omega/\square$ to $7 \Omega/\square$, which is one order of magnitude lower than the PEDOT:PSS electrodes at the same transmittance [16,17]. Top-view scanning electron microscope (SEM) images of the Ag films with and without the Au seed layer are shown in Fig. 2(b). It can be seen that the Ag film with the Au seed layer is more continuous, which results in the lower sheet resistance. Moreover, the more continuous film can reduce light scattering and contribute to the higher transmittance.

Polymer-fullerene derivative PCDTBT:PC₇₁BM with a high efficiency was used as the absorber layer in the stretchable PSCs. LiF/Al is used as the interfacial modification layer of cathode to match the energy level of PC₇₁BM. We used Ag layer with better ductility as cathode to replace the commonly used Al cathode. A sacrificial layer of NPB covers over the whole sample. The real photographs of the stretchable PSCs at different tensile strains are shown in Fig. 3(a).

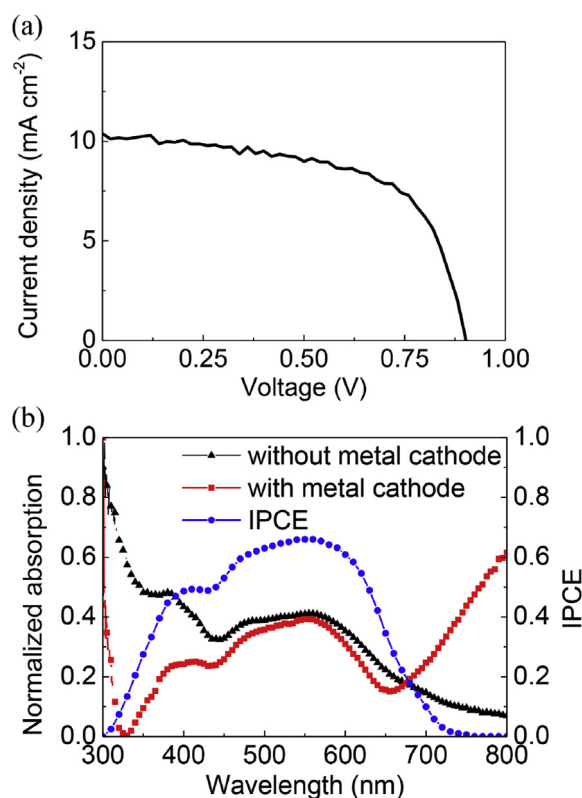


Fig. 4. (a) J–V characteristic curve of the stretchable PSC at 70% tensile strain. (b) Normalized absorption spectra of stretchable PSCs with and without metal cathode and IPCE of the stretchable PSCs at 70% tensile strain.

The maximal tensile strain of about 70% can be achieved. Random bucklings can be observed clearly. The morphology of the device at 0% strain is intuitively displayed in the SEM image (Fig. 3(b)). The bending radius of the bucklings can be as small as tens of micrometer due to the high flexibility of the ultrathin PSCs.

The current density-voltage (J–V) characteristic of the stretchable PSCs under the maximum tensile strain (nearly planar state) is presented in Fig. 4(a). The device performs with $V_{OC} = 0.9 \text{ V}$, $J_{SC} = 10.39 \text{ mA cm}^{-2}$, $FF = 62.0\%$ and $PCE = 5.8\%$. These results are

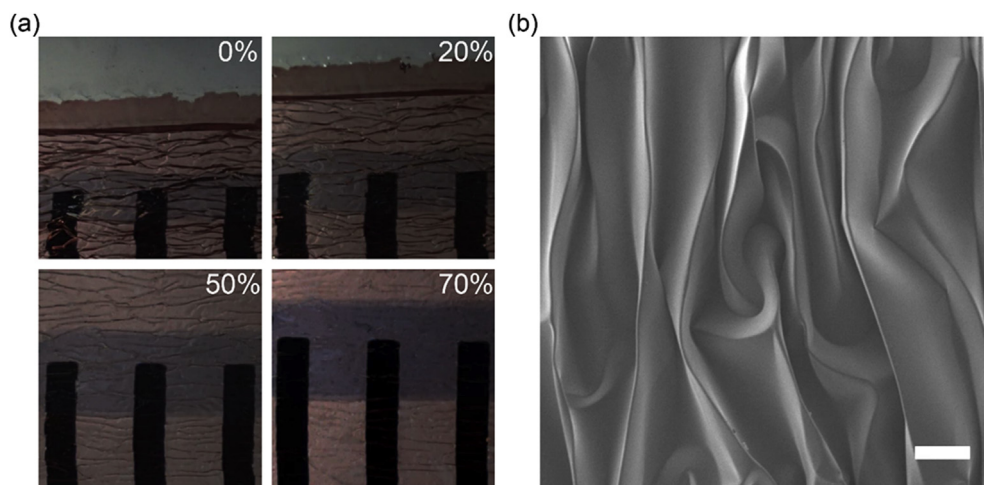


Fig. 3. (a) Photographs of the stretchable PSCs at 0%, 20%, 50% and 70% tensile strains. (b) Top-view SEM image of the stretchable PSC at 0% tensile strain. The scale bar is 200 μm .

comparable to leading bulk heterojunction (BHJ) PSCs with PCDTBT:PC₇₁BM as absorber and ITO as anode [18]. The UV–visible absorption spectras of devices with and without the metallic cathode and incident photon-to-current efficiency (IPCE) spectra are shown in Fig. 4(b). The absorption spectrum covers entire visible spectral range. An enhancement in absorption >650 nm is observed in the device with the metallic Ag cathode compared to that of the device without the metallic cathode, which is caused by the microcavity formed by the two metallic electrodes. The peaks in IPCE spectra are consistent well with the absorption spectra of the device without the cathode and the maximum EQE of 68% is achieved.

The I–V characteristics of the stretchable PSCs at different tensile strains are measured and the results are shown in Fig. 5(a). It is clear that the stretchable PSCs can normally work at each tensile strain. With tensile strain increasing, V_{OC} and FF are almost constant, while the short circuit current I_{SC} presents a linear increasing (Fig. 5(b)). This is because the effective light-absorbing area increases linearly with the increasing of the tensile strain.

The stretchable PSCs tend to breakdown during the buckles forming and stretching-releasing process in case the device's cathode contacted directly with the elastomeric substrate. The cathodes may be damaged by the compressive stress from the elastomer. Here, the 0, 10, 20, 30, 40 nm-thick NPB sacrificial layers were deposited on the cathode films to avoid their contact and improve the mechanical stability of the stretchable PSCs. To investigate the mechanical robustness of the devices, the performance of the stretchable PSCs was measured under the repeated stretching-releasing cycles at tensile strain values between 0% and

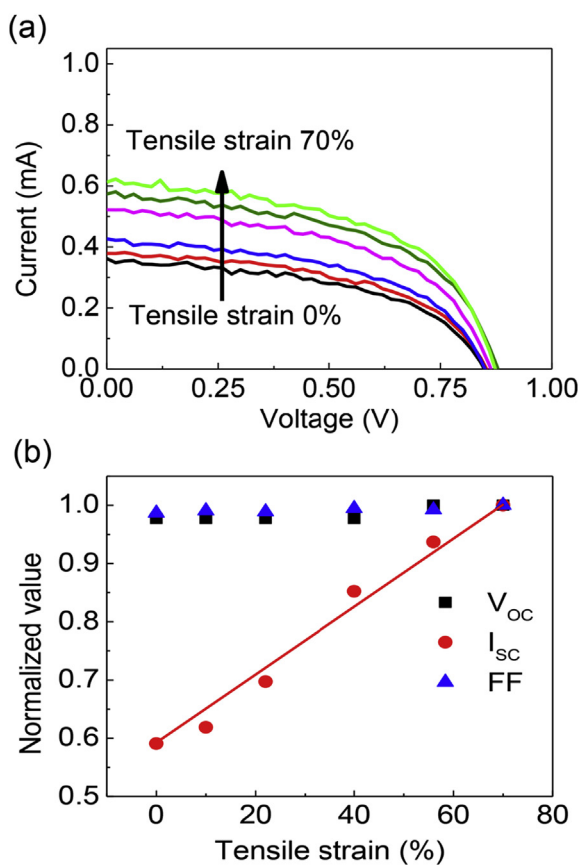


Fig. 5. (a) J–V characteristics of the stretchable PSCs at various tensile strains (0%, 15%, 22%, 40%, 56% and 70%). (b) Dependence of the PSC performance on the various tensile strains. All parameters are normalized to their maximum value.

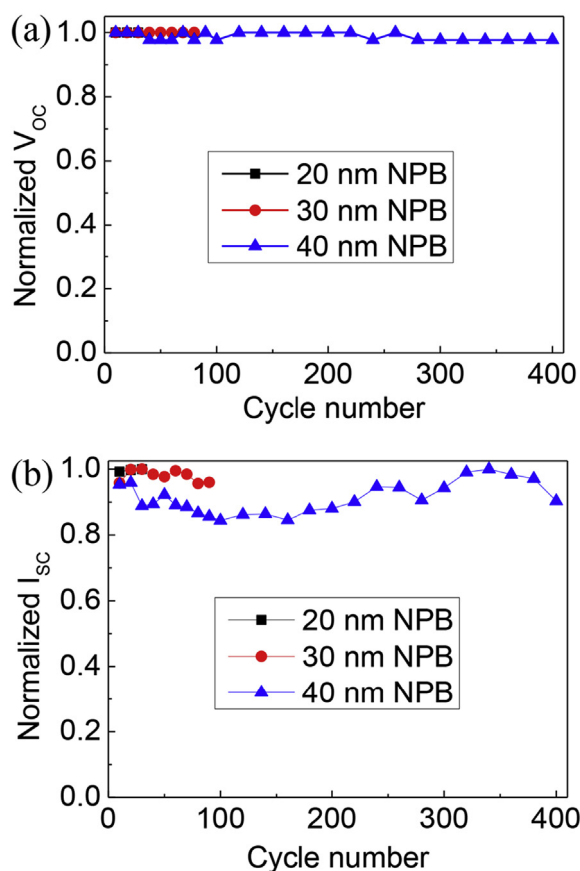


Fig. 6. V_{OC} (a) and I_{SC} (b) vs the stretching cycle number for the stretchable PSCs with 20, 30, 40 nm NPB layer between 0% and 70% strain.

70%. The I–V characteristics at 0% strain were recorded under the solar simulator after every 10 or 20 cycles. The characteristics of V_{OC} and I_{SC} as a function of the cycle number are shown in Fig. 6. In test of cycle stretching, when the thickness of NPB layer was less than or equal to 10 nm, we almost couldn't test performance of devices and the maximum cycle numbers of the PSCs with 20, 30 and 40 nm NPB layers are 30, 90, and 400, respectively. A thicker sacrificial layer benefits stability of device, while, a thicker layer would result in a poor adhesion between the PSC and the elastomeric substrate. The sacrificial layer of NPB film with 40 nm was chosen in this work. The V_{OC} has almost no change after 400 stretching-releasing cycles. A fluctuation of the I_{SC} can be observed, which is within $\pm 13.2\%$ and may be caused by the fluctuation of the effective area during the stretching-releasing cycles.

4. Conclusions

In summary, we demonstrate stretchable PSCs with high efficiency and improved mechanical robustness based on the random buckling process. A power conversion efficiency of 5.8% under 70% strain has been achieved for the stretchable PSCs, which is by far the highest efficiency among the reported stretchable PSCs. A NPB sacrificial layer was deposited on cathode to avoid direct contact between the PSCs and elastomeric substrate and consequently improve its mechanical robustness. As a result, the stretchable PSCs exhibit small fluctuations in performance after 400 stretching-releasing cycles. This is an important step towards producing fully stretchable PSCs for applications in wearable electronics.

Acknowledgements

The authors gratefully acknowledge support from the NSFC (Grant Nos. 61675085, 61322402, 61505065, 60605056, and 61590930).

References

- [1] S. Savagatrup, A.D. Printz, T.F. O'Connor, A.V. Zaretski, D.J. Lipomi, Molecularly stretchable electronics, *Chem. Mater* 26 (2014) 3028–3041.
- [2] S.J. Benight, C. Wang, J.B.H. Tok, Z. Bao, Stretchable and self-healing polymers and devices for electronic skin, *Prog. Polym. Sci.* 38 (2013) 1961–1977.
- [3] C. Larson, B. Peele, S. Li, S. Robinson, M. Tataro, L. Beccai, B. Mazzolai, R. Shepherd, Highly stretchable electroluminescent skin for optical signaling and tactile sensing, *Science* 351 (2016) 1071–1074.
- [4] G. Kettlgruber, M. Kaltenbrunner, C.M. Siket, R. Moser, I.M. Graz, R. Schwödiauer, S. Bauer, Intrinsically stretchable and rechargeable batteries for self-powered stretchable electronics, *J. Mater. Chem. A* 1 (2013) 5505.
- [5] H. Wu, S. Kustra, E.M. Gates, C.J. Bettinger, Topographic substrates as strain relief features in stretchable organic thin film transistors, *Org. Electron* 14 (2013) 1636–1642.
- [6] D.J. Lipomi, H. Chong, M. Vosgueritchian, J. Mei, Z. Bao, Toward mechanically robust and intrinsically stretchable organic solar cells: evolution of photovoltaic properties with tensile strain, *Sol. Energy Mater. Sol. Cells* 107 (2012) 355–365.
- [7] B. Park, S.H. Yun, C.Y. Cho, Y.C. Kim, J.C. Shin, H.G. Jeon, Y.H. Huh, I. Hwang, K.Y. Baik, Y.I. Lee, H.S. Uhm, G.S. Cho, E.H. Choi, Surface plasmon excitation in semitransparent inverted polymer photovoltaic devices and their applications as label-free optical sensors, *Light Sci. Appl.* 3 (2014) e222.
- [8] T. Kim, J.H. Kim, T.E. Kang, C. Lee, H. Kang, M. Shin, C. Wang, B. Ma, U. Jeong, T.S. Kim, B.J. Kim, Flexible, highly efficient all-polymer solar cells, *Nat. Commun.* 6 (2015) 8547.
- [9] D.J. Lipomi, B.C. Tee, M. Vosgueritchian, Z. Bao, Stretchable organic solar cells, *Adv. Mater* 23 (2011) 1771–1775.
- [10] M. Kaltenbrunner, M.S. White, E.D. Glowacki, T. Sekitani, T. Someya, N.S. Sariciftci, S. Bauer, Ultrathin and lightweight organic solar cells with high flexibility, *Nat. Commun.* 3 (2012) 770.
- [11] S. Schubert, J. Meiss, L. Müller-Meskamp, K. Leo, Improvement of Transparent Metal Top Electrodes for organic solar cells by introducing a high surface energy seed layer, *Adv. Energy Mater* 3 (2013) 438–443.
- [12] J. Zou, C.Z. Li, C.Y. Chang, H.L. Yip, A.K. Jen, Interfacial engineering of ultrathin metal film transparent electrode for flexible organic photovoltaic cells, *Adv. Mater* 26 (2014) 3618–3623.
- [13] D. Zhao, C. Zhang, H. Kim, L.J. Guo, High-performance Ta₂O₅/Al-doped Ag electrode for resonant light harvesting in efficient organic solar cells, *Adv. Energy Mater* 5 (2015) 1500768.
- [14] Y. Chen, L. Shen, W. Yu, Y. Long, W. Guo, W. Chen, S. Ruan, Highly efficient ITO-free polymer solar cells based on metal resonant microcavity using WO₃/Au/WO₃ as transparent electrodes, *Org. Electron* 15 (2014) 1545–1551.
- [15] R. Ding, J. Feng, X.-L. Zhang, W. Zhou, H.-H. Fang, Y.-F. Liu, Q.-D. Chen, H.-Y. Wang, H.-B. Sun, Fabrication and characterization of organic single Crystal-Based Light-Emitting Devices with Improved contact between the metallic electrodes and crystal, *Adv. Funct. Mater* 24 (2014) 7085–7092.
- [16] M. Vosgueritchian, D.J. Lipomi, Z. Bao, Highly conductive and transparent PEDOT: PSS films with a fluorosurfactant for stretchable and flexible transparent electrodes, *Adv. Funct. Mater* 22 (2012) 421–428.
- [17] J.G. Tait, B.J. Worfolk, S.A. Maloney, T.C. Hauger, A.L. Elias, J.M. Buriak, K.D. Harris, Spray coated high-conductivity PEDOT: PSS transparent electrodes for stretchable and mechanically-robust organic solar cells, *Sol. Energy Mater. Sol. Cells* 110 (2013) 98–106.
- [18] V.S. Murugesan, S. Ono, N. Tsuda, J. Yamada, P.-K. Shin, S. Ochiai,

Characterization of organic thin film solar cells of PCDTBT:PC₇₁BM prepared by different mixing ratio and effect of hole transport layer, *Int. J. Photoenergy* 2015 (2015) 1–8.



Rui Ma received the B.S. degree in electronics science and technology in 2014 from the College of Electronic Science and Engineering, Jilin University, China, where he is currently pursuing the Master's degree. His current research interests are in the area of stretchable organic optoelectronic devices.



Jing Feng received the B.S. and Ph. D. degrees in microelectronics and solid-state electronics from Jilin University, Changchun, China, in 1997 and 2003, respectively. She worked as a Postdoctoral Researcher at RIKEN, Japan, from 2003 to 2006. She joined Jilin University in 2006, where she is currently a Professor of College of Electronic Science and Engineering and State Key Laboratory on Integrated Optoelectronics. Her research interests include organic optoelectronic devices and stretchable electronics. She has published over 50 scientific papers in academic journals.



Da Yin received the B.S. degree in microelectronics in 2011 from the College of Electronic Science and Engineering, Jilin University, China, where he is currently pursuing the Ph.D. degree. His current research interests are in the area of organic optoelectronic devices and stretchable electronics.



Hong-Bo Sun received the Ph.D. degree from Jilin University, China, in 1996. He worked as a Postdoctoral Researcher at the University of Tokushima from 1996 to 2000, and then as an Assistant Professor at Osaka University, Japan. He became a Project Leader in 2001. In 2005, he became a Professor (Changjiang Scholar) at Jilin University. His research is focused on laser micro-nanofabrication, and its application in microoptics, micromachines, microfluids, and microsensors. Dr. Sun was awarded by the Optical Science and Technology Society in 2002, and won an Outstanding Young Scientist Award issued by the minister of MEXT (Japan) in 2006.